Journal of Hazardous Materials 211–212 (2012) 62–67

Contents lists available at SciVerse ScienceDirect

Journal of Hazardous Materials

journal homepage: www.elsevier.com/locate/jhazmat

ZnS nanocrystals and nanoflowers synthesized by a green chemistry approach: Rare excitonic photoluminescence achieved by the tunable molar ratio of precursors

Ningru Xiao [1], Quanqin Dai [1], Yingnan Wang, Jiajia Ning, Bingbing Liu, Guangtian Zou, Bo Zou *

State Key Laboratory of Superhard Materials, Jilin University, 2699 Qianjin Street, Changchun, Jilin Province 130012, PR China

ARTICLE INFO

Article history:
Received 1 June 2011
Received in revised form 3 November 2011
Accepted 3 November 2011
Available online 10 November 2011

Keywords:
Green chemistry
ZnS
Excitonic emission
Nanocrystals
Nanoflowers

ABSTRACT

In the present work, we demonstrated a simple and green synthesis route for shape-controlled ZnS nanocrystals, where only environmentally benign chemicals, namely sulfur, zinc oxide and olive oil, were employed. By controlling the experimental conditions, we were able to tune the band edge and trap state photoluminescences of ZnS nanocrystals and obtain pure excitonic photoluminescence that was rarely observed in literature. The trap state emission was derived from sulfur vacancies and would be eliminated when an excess of sulfur was used during the synthesis. Additionally, the morphology of ZnS nanocrystals could be tuned to appear like flowers, where the formation mechanism was systematically discussed.

1. Introduction

Recently, photoluminescent semiconductor nanocrystals (NCs) have received significant attention because of their size- and shape-dependent physical and chemical properties [1]. They are employed for various applications including biomedical tags and diagnostics [2], light emitting diodes [3,4], lasers [5,6] and solar cell [7]. However, many benefits of the applications are linked to a doubtful future, due to concerns about the harm to our environment and living organism [8]. Therefore, great care and foresight should be taken to ensure that the synthesis of high-quality NCs are safe and effective [9,10], where green chemistry approaches are increasingly being used [11,12].

Zinc sulfide (ZnS) is an environmentally benign semiconductor with a wide direct band gap (3.6 eV). It is an attractive material and has a wide range of applications covering flat panel displays, nonlinear optical devices, ultraviolet sensors, lasers, and so forth [13–16]. The fast development of nanoscience and nanotechnology makes ZnS nanomaterials successfully synthesized into a variety of morphologies, such as nanoparticles [17–19], nanowires [20,21], nanorods [22,23], nanobelts [13], nanosheets [15] and more complicated nanostructures [24–26]. In these cases, they exhibit various optical properties because of the high sensitivity to size, shape, and synthetic environment [27–29]. Manipulation of obtaining desired optical spectra of ZnS NCs is significant for their applications. However, rather than the report of their excitonic emission in the ultraviolet (UV) region, most reports described the broad emission in the visible range. Such broad emission was related to the considerable trapped states of ZnS NCs. Pure excitonic emission with trap states excluded was challenging for ZnS NCs. Wageh et al. enhanced the band gap emission by increasing the reflux time of growth solution for a long time (up to 10 h) at a temperature of 1–2 °C; however, the weak emission tail derived from trap states also existed [30]. Li et al. made significant contributions to the excitonic emission of ZnS NCs, which still mixed with deep trap emission [31]. The reason that the pure band edge emission of ZnS NCs was rarely obtained is because of the loss of excitons into their trap states [32]. The competition between the band edge emission and trap state emission limits the application of ZnS NCs as UV/blue emitters. Therefore, there still is an apparent lack of a good solution, especially a green chemistry approach, to prepare ZnS NCs with pure excitonic emission.

In our present preparation method, we used nontoxic chemicals (sulfur, zinc oxide and olive oil) to synthesize zinc blende ZnS NCs. Different molar ratios of precursors were used and found to play a significant effect on the photoluminescence (PL) properties of ZnS NCs. When an excess of sulfur precursors was used during the synthesis, the trap state emission originated from sulfur vacancies would be eliminated and hence pure excitonic emission was

* Corresponding author.
E-mail address: zoubo@jlu.edu.cn (B. Zou).
[1] These authors contributed equally to this work.

0304-3894/$ – see front matter © 2011 Elsevier B.V. All rights reserved.
doi:10.1016/j.jhazmat.2011.11.020

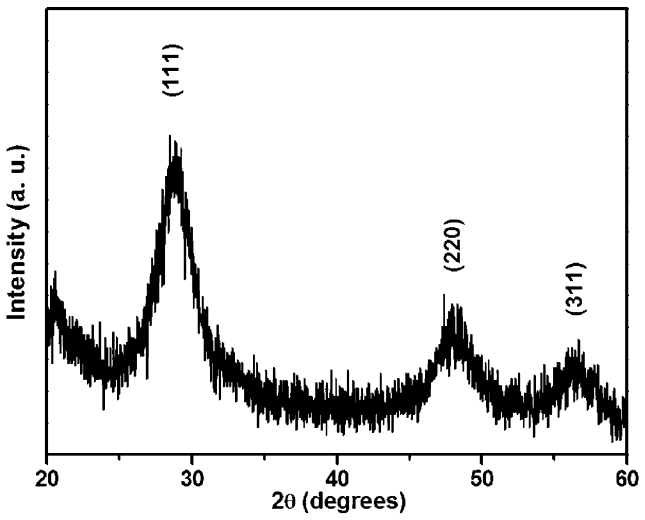

Fig. 1. XRD patterns of the ZnS NCs synthesized with a S:Zn molar ratio of 1:2.

observed. Comparatively, a large excess of Zn precursors led to the formation of three-dimensional (3D) ZnS nanoflowers, where the formation mechanism was systematically discussed.

2. Experimental details

2.1. Materials

ZnO (99.9%) and S (99.9%) were purchased from Sinopharm Chemical Reagent Co., Ltd. Olive oil was ordered from Fluka (Product no. 75357). Acetone (analytical grade), chloroform (analytical grade) were purchased from commercial sources. All chemicals were used as received without further purification.

2.2. Synthesis of monodisperse ZnS NCs

Typically, S solution was obtained by dissolving 0.2 mmol of S in 1 mL of olive oil at 100 °C for 0.5 h and then cooled down to room temperature. Meanwhile, a mixture of ZnO powder (0.4 mmol) and olive oil (5.0 mL) was added to a 50 mL three-neck flask that was connected to a Schlenk line. The mixture was heated to 330 °C under nitrogen flow, where ZnO powder was completely dissolved under stirring. At this temperature, the S solution was swiftly injected into the vigorously stirred reaction solution, which was followed by the drop of temperature to ~310 °C. At different reaction moments, aliquots were taken from the reaction flask and immediately mixed with cold acetone to quench their reaction. After purified by centrifugation, the prepared ZnS NCs could be re-dispersed in organic solvents such as hexanes, toluene, or chloroform. In the above reaction, the initial molar ratio of S:Zn is 1:2. Reactions with other molar ratios were carried out as well.

2.3. Synthesis of nanoflowers

This synthesis was the same as above, except that a large excess of ZnO power (0.8 mmol) was used.

2.4. Characterization

All measurements were performed at room temperature. Ultraviolet–visible absorption (UV–vis) and photoluminescence spectra were measured by a Shimadzu UV-3150 spectrometer and a Photon Technology International photoluminescence, respectively. The photoluminescence quantum yields (PL QYs) of ZnS

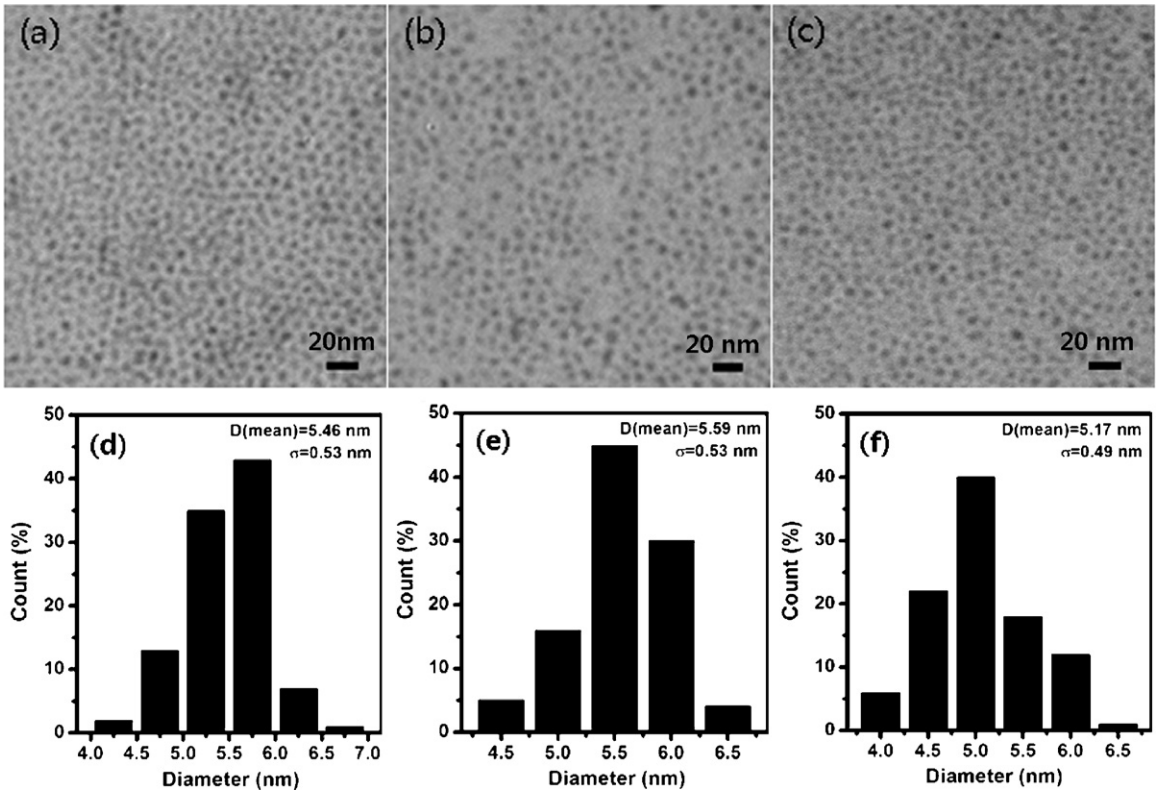

Fig. 2. TEM images of the ZnS NCs synthesized with different S:Zn molar ratios (a) S:Zn = 1:2, (b) S:Zn = 1:1 and (c) S:Zn = 2:1. (d), (e) and (f) are the corresponding size-distribution histograms of above TEM images, respectively.

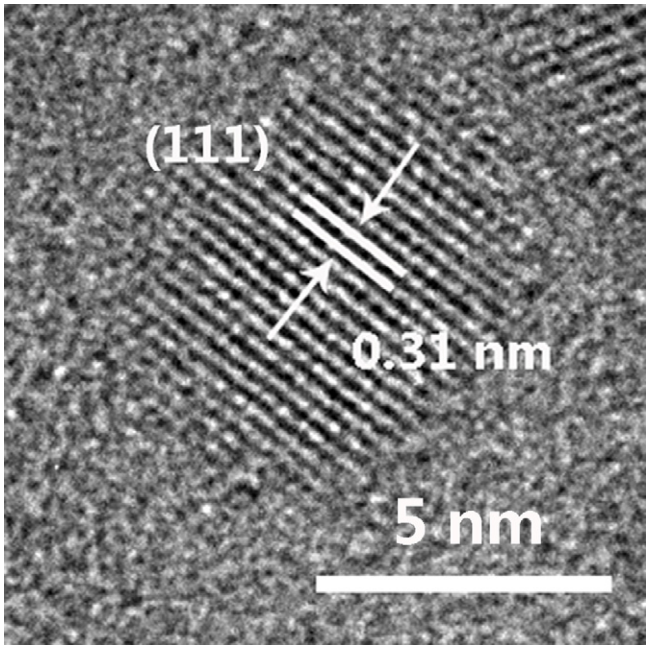

Fig. 3. HRTEM image of ZnS NC synthesized with a S:Zn molar ratio of 1:2.

NCs were measured using L-tyrosine as a standard (14% in water). X-ray diffraction (XRD) patterns were recorded via a Shimadzu XRD-6000 working with a Cu K_α target. Transmission electron microscopy (TEM) images were obtained by a Hitachi H-8100IV microscope operated at 200 kV. High-resolution transmission electron microscopy (HRTEM) images were obtained by a JEM-2100F microscope operated at 200 kV.

3. Results and discussion

The crystalline phase of the resulting products was investigated using powder XRD. As shown in Fig. 1, three obvious peaks were observed, corresponding to the (1 1 1), (2 2 0), and (3 1 1) planes of cubic (zinc-blende) ZnS. These peaks showed broad features, meaning small crystalline sizes. This was consistent with the TEM observation in Fig. 2. TEM studies showed that no matter which of the S:Zn molar ratios (1:2, 1:1, and 2:1) was used in our green synthesis, the resulting products looked dot-shaped and uniform (Fig. 2a–c); the standard deviations of size distributions were smaller than 10% (Fig. 2d–f). The HRTEM image of individual NC showed clear lattice fringes with a spacing of $d = 0.31$ nm (Fig. 3), corresponding to the (1 1 1) lattice plane of the zinc-blende structure.

The size-dependent optical properties of ZnS NCs could be monitored through the temporal evolution of absorption spectra. Fig. 4a displayed the UV–vis absorption spectra of ZnS NCs taken at different intervals of the typical synthesis (S:Zn = 1:2). Their absorption peaks were all much shorter than that of bulk ZnS (344 nm), which was attributable to the quantum confinement effect. The ZnS NCs grew fast after S precursors were injected into the reaction solution. As the reaction proceeded to about 20 s, the relatively sharp absorption peak located at 295 nm was observed. The absorption peak red shifted to 307 nm when the reaction time increased to 1 h, which indicated the growth of ZnS NCs and their size-dependent quantum confinement effect. As displayed in Fig. 4a, the absorption peaks at the early stage of reaction could be obviously recognized. However, at the prolonged stage of reaction, the absorption peaks became unobvious. This was because the nanocrystal growth underwent a process called "defocusing" [33]. This process represented the broadening of nanocrystal size distributions, which could be visually reflected by the broad and unobvious absorption peaks.

The PL properties of the above products could be seen in Fig. 4b. Two emission regions in the UV range and visible range, respectively, were observed for all samples taken at reaction times from 20 s to 1 h. The narrow emission at shorter wavelengths corresponded to the band edge (or excitonic) emission; the broad emission at longer wavelengths was attributed to the trap-related emission. As reported previously, the excitonic emission of ZnS NCs was commonly accompanied by their trap-related emission due to the loss of excitons into trap states [27]. Such trap states were derived from zinc and sulfur vacancies. The trap state emission related to zinc vacancies was reported to exhibit a broad peak located at ~480 nm [34], while the broad peak of our ZnS NCs located at ~420 nm was commonly assigned to sulfur vacancies [27].

Tuning defect emission was previously observed in ZnS nanostructures [28], showing the difficulty or even impossibility to obtain pure excitonic emission from ZnS NCs. The above results, however, told us the filling of sulfur vacancies should be an effective strategy to diminish or eliminate the defect-related emission in our case. Thus, we increased the sulfur proportion during the reaction. As shown in Fig. 5a, the initial molar ratio of S:Zn was increased to 1:1 from its original 1:2. Although the optical spectra still consisted of two emission regions that were similar to those in Fig. 4b, the relative intensity of trap state emission to excitonic emission was found to decrease with the increase of sulfur proportions. For example, when the initial S:Zn ratio in the reaction was increased from 1:2 to 1:1, the relative intensity ratio of defect-related emission to excitonic emission decreased from ~4.8 to ~2.5 at 20 s of the reaction interval. Such intensity ratios kept decreasing as the reaction lasted longer. On the basis of such positive facts, we were encouraged to further increase the sulfur proportion, aiming to completely eliminate the trap state emission of ZnS NCs. When the initial molar ratio of S:Zn was increased to 2:1, the band edge emission and trap state emission further increased and decreased, respectively. More encouragingly, the broad emission in the visible range was completely quenched at 10 min or longer, where only the pure excitonic emission was observed in the UV region (Fig. 5b). Consequently, we succeeded to prepare ZnS NCs with pure excitonic emission. Although some papers reported excitonic emission from ZnS NCs, trap-related emission existed more or less [30,35]. In our green chemistry approach, the PL properties could be manipulated by simply adjusting the molar ratio of precursors, in which we were able to obtain pure excitonic emission in a relatively short reaction time (such as 10 min).

Due to the existence of sulfur vacancies, extra trap states would be introduced and thus form the trapping center to capture electrons quickly. These captured electrons contributed only to the trap state emission, while the excited electrons that not were captured by trap states resulted in excitonic emission. With the increase of sulfur, more sulfur vacancies will be filled and thus trapping centers would be fewer [34,36]. An excess of sulfur could effectively fill sulfur vacancies, where trap state emission would be eliminated and accordingly pure excitonic emission became possible (Fig. 5b).

The PL quantum efficiency of our resulting NCs was not high (below 10%), consistent with the reported efficiency of Zn-related NCs with fatty acids as the ligand [31]. Fig. 6 was used to exhibit the temporal evolution of PL QYs of ZnS NCs at different molar ratios of precursors. With the initial S:Zn ratios equal to 1:2 and 1:1, respectively, slightly increased PL QY values over reaction time were obtained (Fig. 6a and b). Furthermore, when the trap state emission was gradually eliminated, the PL QY had an obvious increase, as shown in Fig. 6c. These temporal evolutions of PL QYs demonstrated that, with the increase of S:Zn molar ratio, the trap-related

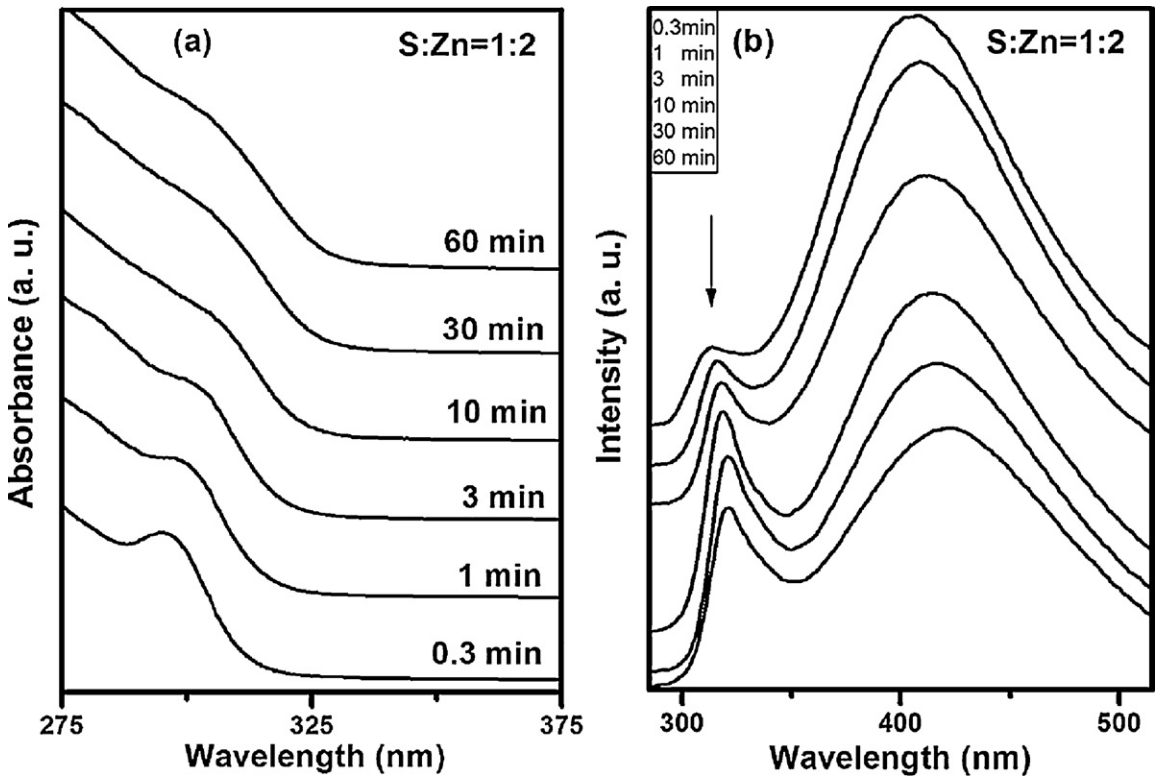

Fig. 4. Temporal evolution of (a) UV–vis and (b) PL spectra of the ZnS NCs synthesized with a S:Zn molar ratio of 1:2.

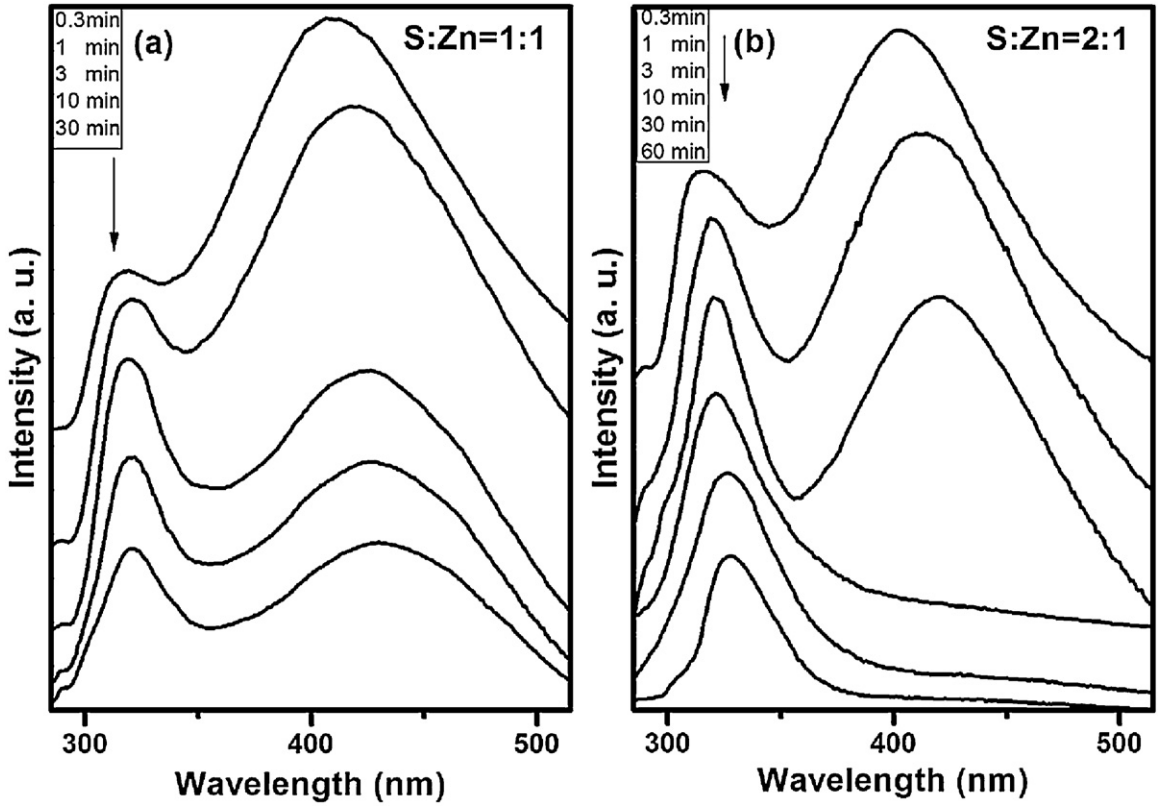

Fig. 5. Temporal evolution of PL spectra of the ZnS NCs obtained with different molar ratios (a) S:Zn = 1:1 and (b) S:Zn = 2:1.

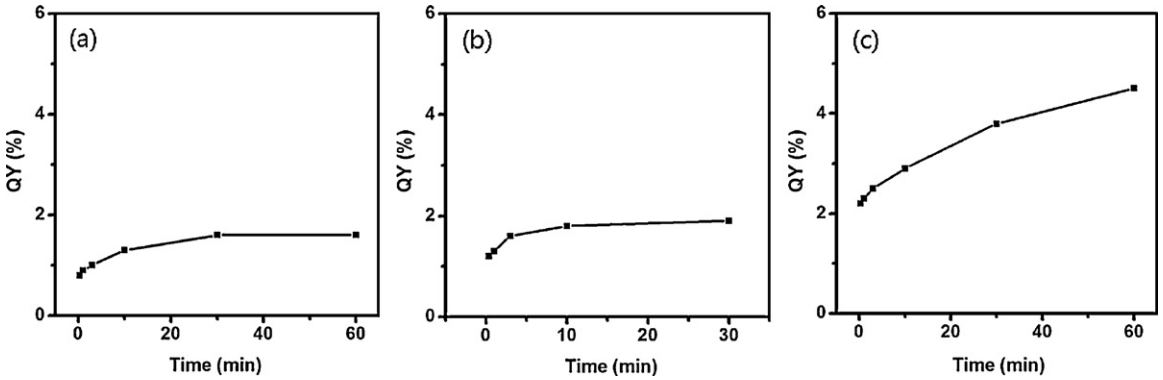

Fig. 6. Temporal evolution of PL QYs of ZnS NCs synthesized with different S:Zn molar ratios (a) S:Zn = 1:2, (b) S:Zn = 1:1, and (c) S:Zn = 2:1.

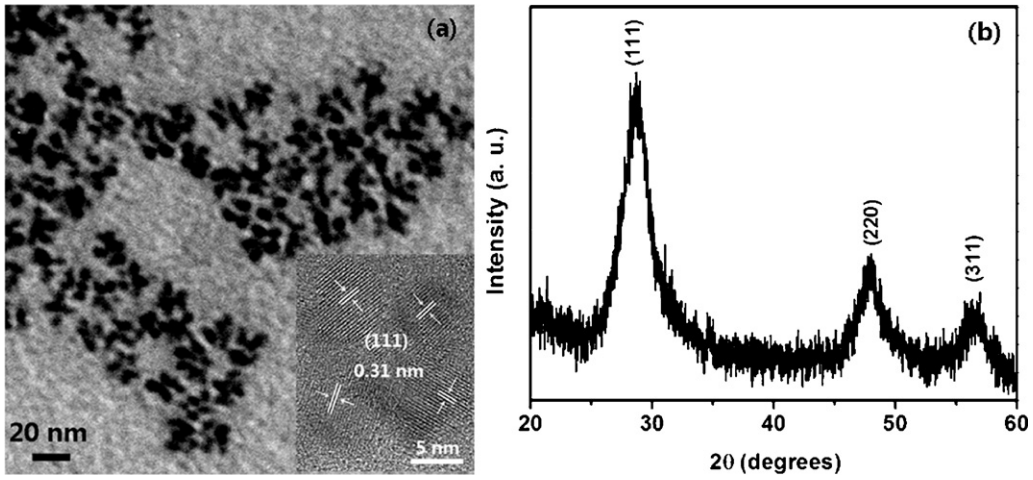

Fig. 7. (a) TEM image (inset: HRTEM image) and (b) XRD patterns of the as-prepared ZnS nanoflowers.

emission could eventually decrease to zero, while the excitonic emission kept increasing.

Much effort has been made to control the morphology of ZnS NCs [37]. However, 3D NCs, such as nanoflowers, have been rarely reported. The morphologies of our as-synthesized ZnS NCs could be tuned to look like nanoflowers, when the Zn precursor was initially increased (0.8 mmol). Fig. 7a presented the TEM image of flower-like ZnS. It seemed that the resulting nanoflowers consisted of some aggregated ZnS NCs, and were further investigated by a typical HRTEM image (inset of Fig. 7a). The lattice fringes with a spacing of $d = 0.31$ nm corresponded to the (1 1 1) lattice plane of the zinc blende structure. The typical XRD patterns of the as-prepared nanoflowers could be observed in Fig. 7b, where three peaks corresponded to the (1 1 1), (2 2 0), and (3 1 1) planes. It indicated these nanoflowers possessed a pure zinc blende structure, similar to that of the individual ZnS NCs. All the XRD patterns of nanoflowers also showed the similar size broadening to the individual ZnS NCs, indicating both the NC-composed nanoflowers and the individual NCs possessed similar crystalline sizes. This further revealed that individual NCs attached closely to form nanoflowers.

Earlier, Peng and co-workers [38,39] observed the formation of nanoflowers, where the limited ligand protection (LLP) was employed to explain the formation mechanism. A high-enough concentration of surface ligands should be used to passivate and maintain dot-shaped NCs. However, when the surface ligands added were not sufficient to protect individual NCs, namely LLP, they would become unstable and attach on some unprotected surfaces to form 3D nanoflowers. As shown above, LLP was achieved through both decreasing the concentration of surface ligands and maintaining the amount of precursors. Similarly, increasing precursors and maintaining surface ligands should reach the same effect. As shown in Fig. 7a, simply increasing the initial amount (0.8 mmol) of Zn precursors and maintaining the other conditions resulted in ZnS nanoflowers. Thus, we provided here an alternative simple route to reach LLP for the formation of ZnS nanoflowers.

4. Conclusion

In conclusion, we synthesized dot- and flower-shaped ZnS NCs through a green chemistry approach. The commonly existing trap state emission of ZnS NCs could be completely eliminated in appropriate conditions, where only pure excitonic emission was observed. Without trap state emission, our prepared ZnS NCs were more likely to serve as a potential UV emitter. Moreover, we offered an alternative scheme to achieve the LLP, resulting in 3D nanoflowers.

Acknowledgements

This work was supported by NSFC (Nos. 21073071, and 51025206), the National Basic Research Program of China (No. 2011CB808200 and No. 2007CB808000) and Graduate Innovation Fund of Jilin University (No. 20101056).

References

[1] X.G. Peng, L. Manna, W.D. Yang, J. Wickham, E. Scher, A. Kadavanich, A.P. Alivisatos, Shape control of CdSe nanocrystals, Nature 404 (2000) 59–61.

[2] L.L. Wang, H.Z. Zheng, Y.J. Long, M. Gao, J.Y. Hao, J. Du, X.X. Mao, D.B. Zhou, Rapid determination of the toxicity of quantum dots with luminous bacteria, J. Hazard. Mater. 177 (2010) 1134–1137.
[3] V.L. Colvin, M.C. Schlamp, A.P. Alivisatos, Light-emitting diodes made from cadmium selenide nanocrystals and a semiconducting polymer, Nature 370 (1994) 354–357.
[4] J. Lee, V.C. Sundar, J.R. Heine, M.G. Bawendi, K.F. Jensen, Full color emission from II–VI semiconductor quantum dot–polymer composites, Adv. Mater. 12 (2000) 1102–1105.
[5] V.I. Klimov, A.A. Mikhailovsky, S. Xu, A. Malko, J.A. Hollingsworth, C.A. Leatherdale, H.J. Eisler, M.G. Bawendi, Optical gain and stimulated emission in nanocrystal quantum dots, Science 290 (2000) 314–317.
[6] M. Kazes, D.Y. Lewis, Y. Ebenstein, T. Mokari, U. Banin, Lasing from semiconductor quantum rods in a cylindrical microcavity, Adv. Mater. 14 (2002) 317–321.
[7] W.U. Huynh, X.G. Peng, A.P. Alivisatos, CdSe nanocrystal rods/poly(3-hexylthiophene) composite photovoltaic devices, Adv. Mater. 11 (1999) 923–927.
[8] C. Feigl, S.P. Russo, A.S. Barnard, Safe, stable and effective nanotechnology: phase mapping of ZnS nanoparticles, J. Mater. Chem. 20 (2010) 4971–4980.
[9] H.W. Wang, X.J. Xu, J.R. Zhang, C.Z. Li, A cost-effective co-precipitation method for synthesizing indium tin oxide nanoparticles without chlorine contamination, J. Mater. Sci. Technol. 26 (2010) 1037–1040.
[10] G.J. Xiao, Q.F. Dong, Y.N. Wang, Y.M. Sui, J.J. Ning, Z.Y. Liu, W.J. Tian, B.B. Liu, G.T. Zou, B. Zou, One-step solution synthesis of bismuth sulfide (Bi2S3) with various hierarchical architectures and their photoresponse properties, RSC Adv., doi:10.1039/c1ra00289a.
[11] P. Raveendran, J. Fu, S.L. Wallen, Completely "Green" synthesis and stabilization of metal nanoparticles, J. Am. Chem. Soc. 125 (2003) 13940–13941.
[12] Q.Q. Dai, N.R. Xiao, J.J. Ning, C.Y. Li, D.M. Li, B. Zou, W.W. Yu, S.H. Kan, H.Y. Chen, B.B. Liu, G.T. Zou, Synthesis and mechanism of particle- and flower-shaped ZnSe nanocrystals: green chemical approaches toward green nanoproducts, J. Phys. Chem. C 112 (2008) 7567–7571.
[13] X.S. Fang, Y. Bando, M.Y. Liao, U.K. Gautam, C.Y. Zhi, B. Dierre, B.D. Liu, T.Y. Zhai, T. Sekiguchi, Y. Koide, D. Golberg, Single-crystalline ZnS nanobelts as ultraviolet-light sensors, Adv. Mater. 21 (2009) 2034–2039.
[14] X.S. Fang, Y. Bando, C.H. Ye, G.Z. Shen, D. Golberg, Shape- and size-controlled growth of ZnS nanostructures, J. Phys. Chem. C 111 (2007) 8469–8474.
[15] X.S. Fang, C.H. Ye, L.D. Zhang, Y.H. Wang, Y.C. Wu, Temperature-controlled catalytic growth of ZnS nanostructures by the evaporation of ZnS nanopowders, Adv. Funct. Mater. 15 (2005) 63–68.
[16] X.S. Fang, Y. Bando, D. Golberg, Recent progress in one-dimensional ZnS nanostructures: syntheses and novel properties, J. Mater. Sci. Technol. 24 (2008) 512–519.
[17] S.H. Choi, K. An, E.G. Kim, J.H. Yu, J.H. Kim, T. Hyeon, Simple and generalized synthesis of semiconducting metal sulfide nanocrystals, Adv. Funct. Mater. 19 (2009) 1645–1649.
[18] T. Kuzuya, Y. Tai, S. Yamamuro, K. Sumiyama, Synthesis of copper and zinc sulfide nanocrystals via thermolysis of the polymetallic thiolate cage, Sci. Technol. Adv. Mater. 6 (2005) 84–90.
[19] J. Joo, H.B. Na, T. Yu, J.H. Yu, Y.W. Kim, F.X. Wu, J.Z. Zhang, T. Hyeon, Generalized and facile synthesis of semiconducting metal sulfide nanocrystals, J. Am. Chem. Soc. 125 (2003) 11100–11105.
[20] Y.J. Zhang, H.R. Xu, Q.B. Wang, Ultrathin single crystal ZnS nanowires, Chem. Commun. 46 (2010) 8941–8943.
[21] Z.T. Deng, H. Yan, Y. Liu, Controlled colloidal growth of ultrathin single-crystal ZnS nanowires with magic-size diameter, Angew. Chem. Int. Ed. 49 (2010) 8695–8698.
[22] B.Y. Geng, X.W. Liu, J.Z. Ma, Q.B. Du, L.D. Zhang, Size-dependent optical and electrochemical band gaps of ZnS nanorods fabricated through single molecule precursor route, Appl. Phys. Lett. 90 (2007) 183106.
[23] J.H. Yu, J. Joo, H.M. Park, S. Baik, Y.W. Kim, S.C. Kim, T. Hyeon, Synthesis of quantum-sized cubic ZnS nanorods by the oriented attachment mechanism, J. Am. Chem. Soc. 127 (2005) 5662–5670.
[24] F. Gu, C.Z. Li, S.F. Wang, M.K. Lü, Solution-phase synthesis of spherical zinc sulfide nanostructures, Langmuir 22 (2005) 1329–1332.
[25] L. Hou, F.M. Gao, Phase and morphology controlled synthesis of high-quality ZnS nanocrystals, Mater. Lett. 65 (2011) 500–503.
[26] X.S. Fang, U.K. Gautam, Y. Bando, B. Dierre, T. Sekiguchi, D. Golberg, Multiangular branched ZnS nanostructures with needle-shaped tips: potential luminescent and field-emitter nanomaterial, J. Phys. Chem. C 112 (2008) 4735–4742.
[27] Y.C. Li, X.H. Li, C.H. Yang, Y.F. Li, Ligand-controlling synthesis and ordered assembly of ZnS nanorods and nanodots, J. Phys. Chem. B 108 (2004) 16002–16011.
[28] X.L. Wang, J.Y. Shi, Z.C. Feng, M.R. Li, C. Li, Visible emission characteristics from different defects of ZnS nanocrystals, Phys. Chem. Chem. Phys. 13 (2011) 4715–4723.
[29] S.N. Sarangi, A.M.P. Hussain, S.N. Sahu, Effect of bimodal size distribution on optical properties of CdSe nanocrystals, Curr. Nanosci. 7 (2011) 275–281.
[30] S. Wageh, Z.S. Ling, X.X. Rong, Growth and optical properties of colloidal ZnS nanoparticles, J. Cryst. Growth 255 (2003) 332–337.
[31] L.S. Li, N. Pradhan, Y.J. Wang, X.G. Peng, High quality ZnSe and ZnS nanocrystals formed by activating zinc carboxylate precursors, Nano Lett. 4 (2004) 2261–2264.
[32] H.B. Shen, C.H. Zhou, S.S. Xu, C.L. Yu, H.Z. Wang, X. Chen, L.S. Li, Phosphine-free synthesis of $Zn_{1-x}Cd_xSe/ZnSe/ZnSe_xS_{1-x}$/ZnS core/multishell structures with bright and stable blue-green photoluminescence, J. Mater. Chem. 21 (2011) 6046–6053.
[33] X.G. Peng, J. Wickham, A.P. Alivisatos, Kinetics of II–VI and III–V colloidal semiconductor nanocrystal growth: "focusing" of size distributions, J. Am. Chem. Soc. 120 (1998) 5343–5344.
[34] J.F. Suyver, S.F. Wuister, J.J. Kelly, A. Meijerink, Synthesis and photoluminescence of nanocrystalline ZnS:Mn^{2+}, Nano Lett. 1 (2001) 429–433.
[35] M. Uehara, S. Sasaki, Y. Nakamura, C.G. Lee, K. Watanabe, H. Nakamura, H. Maeda, Controlled synthesis and structural evolutions of ZnS nanodots and nanorods using identical raw material solution, CrystEngComm 12 (2011) 2973–2983.
[36] K. Manzoor, S.R. Vadera, N. Kumar, T. Kutty, Synthesis and photoluminescent properties of ZnS nanocrystals doped with copper and halogen, Mater. Chem. Phys. 82 (2003) 718–725.
[37] X.S. Fang, T.Y. Zhai, U.K. Gautam, L. Li, L.M. Wu, Y. Bando, D. Golberg, ZnS nanostructures: from synthesis to applications, Prog. Mater. Sci. 56 (2011) 175–287.
[38] A. Narayanaswamy, H.F. Xu, N. Pradhan, X.G. Peng, Crystalline nanoflowers with different chemical compositions and physical properties grown by limited ligand protection, Angew. Chem. Int. Ed. 45 (2006) 5361–5364.
[39] A. Narayanaswamy, H.F. Xu, N. Pradhan, M. Kim, X.G. Peng, Formation of nearly monodisperse In_2O_3 nanodots and oriented-attached nanoflowers: hydrolysis and alcoholysis vs pyrolysis, J. Am. Chem. Soc. 128 (2006) 10310–10319.